DOI: 10.1021/ma902080q

Macromolecules
NOTE

Novel Stimuli-Responsive Polyelectrolyte Brushes

F. J. Xu,*,† F. B. Su,‡ S. B. Deng,§ and W. T. Yang*,†

†*State Key Laboratory of Chemical Resource Engineering, Key Laboratory of Carbon Fiber and Functional Polymers, Ministry of Education, College of Materials Science & Engineering, Beijing University of Chemical Technology, Beijing 100029 China,* ‡*State Key Laboratory of Multi-phase Complex System, Institute of Process Engineering, Chinese Academy of Sciences, Beijing, China 100190, and* §*Department of Environmental Science and Engineering, Tsinghua University, Beijing, 100084 China*

Received September 18, 2009; Revised Manuscript Received January 26, 2010

ABSTRACT: Novel stimuli-responsive polyelectrolyte, poly(*N*-benzyl-*N*′-(4-vinylbenzyl)-4,4′-bipyridium dichloride) or P(BpyClCl), brushes were prepared from the benzyl-chloride-immobilized SiO_2 nanoparticles via surface-initiated atom transfer radical polymerization (ATRP). The dicationions (BV^{2+}) of the P(BpyClCl) brushes can be reduced by UV irradiation to become radical monocations ($BV^{+\cdot}$), which can oxidize back to the original BV^{2+} state by exposure to air. The fast switching between dicationic and monocationic states of the P(BpyClCl) brushes on the SiO_2 nanoparticles can be used as the physically controllable means for the reduction of metal ions (such as Au, Pt, and bimetallic Au/Pt ions) without the need for any added metal reduction agents.

Introduction

Considerable attention has been paid to the manipulation and control of polyelectrolyte (electronically charged polymer) brushes because of their relevance and importance to nanotechnology, surface engineering, and biotechnology.[1] Polyelectrolyte brushes are sensitive to ionic strength, pH, and solvent properties because they can undergo a transition between the fully stretched state and the nearly collapsed state.[1a,i,2] This responsive behavior has often been used to design smart surfaces and to achieve control over surface properties, such as wettability. Metal ions (such as $AuCl_4^-$ and $PtCl_6^{2-}$) can be confined within certain polyelectrolyte brushes and subsequent reduction by suitable reagents produces well-defined metal nanoparticles (NPs).[1d,g,2c] It is well known that metal NPs exhibit unique properties as compared with their bulk counterparts and are of importance to application in emerging areas of nanoscience and nanotechnology.[3]

In this work, novel stimuli-responsive polyelectrolyte brushes of poly(*N*-benzyl-*N*′-(4-vinylbenzyl)-4,4′-bipyridium dichloride) or P(BpyClCl) were prepared via surface-initiated atom transfer radical polymerization (ATRP) of *N*-benzyl-*N*′-(4-vinylbenzyl)-4,4′-bipyridium dichloride (BpyClCl) (a monomer containing the light-sensitive viologen moiety) from the benzyl chloride (BCl)-immobilized SiO_2 (SiO_2-BCl) NPs. The dicationions (BV^{2+}) of the P(BpyClCl) brushes can be reduced by UV irradiation to become radical monocations ($BV^{+\cdot}$), which readily oxidize back to BV^{2+} upon air exposure. The fast switching between BV^{2+} and $BV^{+\cdot}$ states of the P(BpyClCl) brushes on the SiO_2 nanaoparticles can be utilized directly, in lieu of metal reducing agents, to decorate the NPs with metal nanodots (< 5 nm) (Scheme 1).

Experimental Section

Surface-Initiated ATRP of BpyClCl from the SiO_2-BCl NPs. The monomer, *N*-benzyl-*N*′-(4-vinylbenzyl)-4,4′-bipyridium dichloride (BpyClCl), was synthesized according to the method reported in the literature.[4] A mixed solution (20 mL) of 4,4′-bipyridine and benzyl chloride (10 mL) (molar ratio, 1.5:1) was stirred vigorously in dimethylformamide (DMF) at 70 °C for 24 h. The precipitate was washed thoroughly by repeated extraction with ether to ensure the complete removal of residual 4,4′-bipyridine and benzyl chloride. About 8 g of the adduct, *N*-benzyl-4-(4-pyridyl)pyridium chloride, was obtained. The adduct was then reacted with 4-vinylbenzyl chloride (VBC) (molar ratio, 1:1.5) in DMF under continuous stirring at 70 °C for 12 h. The yellow precipitate was collected, washed thoroughly by repeated extraction with acetonitrile, and recrystallized from methanol to produce the desired monomer (~9 g), *N*-benzyl-*N*′-(4-vinylbenzyl)-4,4′-bipyridium dichloride (BpyClCl).

For the preparation of the SiO_2-BCl nanoparticles (NPs), SiO_2 NPs (2.0 g) of ~25 nm in diameter, 3.0 g (9.5 mmol) of trichloro(4-chloromethyphenyl)silane (97%), triethylamine (1.2 mL, 8.6 mmol), and 20 mL of dried THF were introduced to a two-necked flask.[5] The reaction mixture was left to stand for 8 h and then exposed to air for another 18 h. After five cycles of ethanol and THF washing and separation by centrifugation, ~1.8 g of the white benzyl chloride (ATRP initiator) immobilized SiO_2 (SiO_2-BCl) particles was obtained. The chlorine concentration was ~1.44 wt % determined from elemental analysis. This chlorine concentration corresponded to ~2.4 benzyl chloride initiators per nm^2 of the particle surface. Details of the preparation and characterization of the SiO_2-BCl particles had been previously described.[5] For the preparation of BpyClCl polymer (P(BpyClCl)) brushes from the SiO_2-BCl NPs, the reaction was carried out using a [BpyClCl (1.0 g)]/[CuCl]/[Bpy] molar feed ratio of 30:1:2 in 6 mL of degassed water at 80 °C in a Pyrex tube containing 0.2 g of the SiO_2-BCl NPs. The reaction was allowed to proceed for 8 h under continuous stirring to produce the SiO_2-*g*-P(BpyClCl) NPs. After the polymerization, the silica particles were subjected to five cycles of dispersion in methanol and centrifugated to remove catalyst complex, unreacted monomers, and possibly untethered polymers. About 0.15 g of SiO_2-*g*-P(BpyClCl) NPs was obtained.

Metal Reduction on the SiO_2-*g*-P(BpyClCl) NP Surfaces. $AuCl_4^-$ and $PtCl_6^{2-}$ were selected as the model metal ions to

*To whom correspondence should be addressed. E-mail: xufj@mail.buct.edu.cn (F.J.X.); yangwt@mail.buct.edu.cn (W.T.Y.).

 Published on Web 02/04/2010

Scheme 1. Schematic Diagram Illustrating the Preparation of P(BpyClCl) Brushes via Surface-Initiated ATRP of BpyClCl from the SiO_2−BCl NPs and of Metal Nanodots on the SiO_2-*g*-P(BpyClCl) Surface

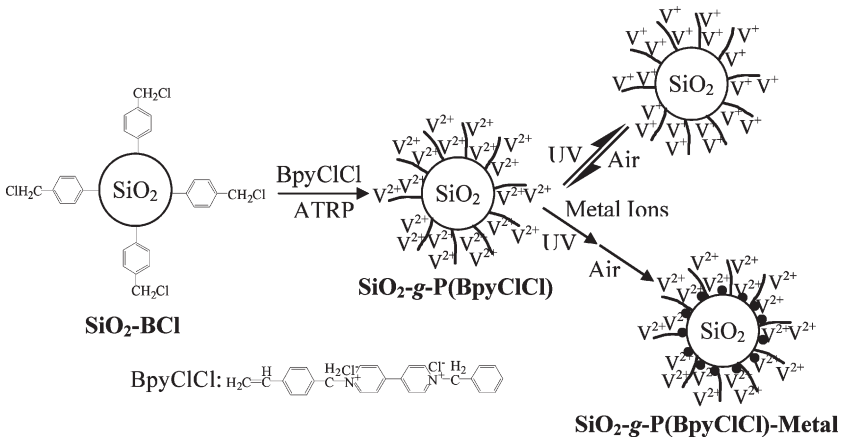

produce the Au, Pt, and bimetallic Au/Pt nanodots. Gold(III) chloride and platinum(IV) chloride solutions (500 ppm) were obtained by diluting the corresponding standard metal salt solutions (1000 ppm) with doubly distilled water. We carried out the reactions of the SiO_2-*g*-P(BpyClCl) NPs with the metal ions by dispersing 1.0 mg/mL of the NPs in the corresponding Au, Pt, and bimetallic Au/Pt solutions (500 ppm) in the Pyrex tubes. The reaction mixtures were purged with argon for 30 min, sealed with a rubber stopper, and exposed to UV irradiation (in a Riko rotary photochemical reactor (RH400-10W) at 20 °C) for 20 min and then exposed to air immediately to produce the metal nanodots-decorated SiO_2-*g*-P(BpyClCl)-Au, SiO_2-*g*-P(BpyClCl)-Pt, and SiO_2-*g*-P(BpyClCl)-Au/Pt NPs, respectively. After the metal reduction reaction, purification of NPs by centrifugation was carried out. Five cycles of NP dispersion in doubly distilled water, followed by centrifugation, were carried out.

Characterization. The X-ray photoelectron spectroscopy (XPS) measurements were performed on a Kratos AXIS HSi spectrometer using a monochromatized Al Kα X-ray source (1486.6 eV photons) and procedures similar to those previously described.[6] The morphology of nanoparticles was characterized on a JEOL JEM 2010F field-emission transmission electron microscope operating at an acceleration voltage of 100 kV. The particle sizes of SiO_2-*g*-P(BpyClCl) NPs were measured using a Zetasizer Nano ZS90 (Malvern Instruments, Southborough, MA) with a laser of 633 nm wavelength at a 173° scattering angle. The size measurement using 3 mg/mL NP solution was performed at 25 °C in triplicate. The Z-average hydrodynamic diameters of the particles were given by the Zetasizer.

Results and Discussion

P(BpyClCl) Brushes via Surface-Initiated ATRP from the SiO_2−BCl NPs. The BpyClCl monomer contains the light-sensitive viologen moiety.[7,8] Figure S1 of the Supporting Information shows the UV−visible absorption spectra of aqueous BpyClCl solution (before irradiation, after 20 min irradiation, and 1 min bleaching in air). No absorption bands were observed in the wavelength range from 400 to 800 nm before irradiation. However, upon photoirradiation of the degassed suspension for 20 min, the solution turned faint blue from pale yellow. Two obvious absorption bands appear at ∼503 and 610 nm, with the one at 503 nm attributable to the dimer form being more intense than the band at 610 nm. The emergence of the typical bands confirms the formation of viologen radical cations ($BV^{+\cdot}$). The above characteristics are consistent with the $BV^{+\cdot}$ of benzyl viologen.[7] The formation of $BV^{+\cdot}$ is caused by the transfer of an electron from the counteranion to the viologen dication

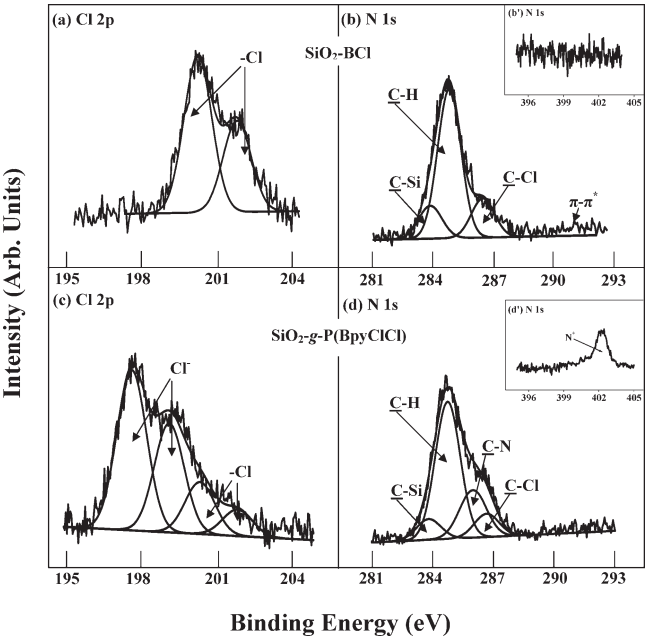

Figure 1. Cl 2p, C 1s, and N 1s core-level spectra of the (a,b,b′) SiO_2−BCl and (c,d,d′) SiO_2-*g*-P(BpyClCl) NPs.

(BV^{2+}). The viologen $BV^{+\cdot}$ readily oxidizes back to BV^{2+} when exposed to air (Scheme S1, Supporting Information).[7,8] Therefore, the blue coloration and typical absorption bands of the BpyClCl solution faded immediately upon exposure to air for 1 min.

The poly(*N*-benzyl-*N*′-(4-vinylbenzyl)-4,4′-bipyridium dichloride) or P(BpyClCl) brushes were prepared via surface-initiated ATRP of BpyClCl from the benzyl chloride (BCl)-immobilized SiO_2 NPs (SiO_2−BCl NPs). The SiO_2−BCl NPs were obtained through the coupling reactions of the chlorosilyl groups of trichloro(4-chloromethyphenyl)silane with the silanol groups of the silica particles of ∼25 nm in diameter. The field emission scanning electron microscopy (FESEM) image (Figure S2, Supporting Information) of the resultant SiO_2−BCl NPs shows that the initiator-immobilized silica NPs still remain segregated or unagglomerated. The XPS Cl 2p core-level spectrum (binding energy (BE) of ∼200 eV,[9] Figure 1a) of the SiO_2−BCl NPs indicates that the BCl ATRP initiators have been successfully immobilized on the silica surfaces. The corresponding C 1s core-level spectrum (Figure 1b) can be curve-fitted with three peak components having BEs at about 283.9, 284.6, and 286.3 eV,

attributable to the C-Si, C-H, and C-Cl species, respectively.[6,9] The $\pi-\pi^*$ shakeup satellite associated with the aromatic ring of BCl is also discernible at the BE of ~291 eV. The appearance of the C-Si and C-Cl species as well as the $\pi-\pi^*$ shakeup satellite further confirms the presence of BCl ATRP initiators on the SiO_2 NPs. A chlorine content of ~1.44 wt % for the SiO_2-BCl nanospheres from elemental analysis has been reported in our previous work.[5] The corresponding surface benzyl chloride initiator concentration is ~2.4 initiators/nm^2 (F). On the basis of the average cross-sectional area (A) of ~2 nm^2 for the vinyl and styrene polymer brushes prepared via ATRP,[6b,10] the surface initiator efficiency of the present system ($1/FA$) is estimated to be ~21%.

The SiO_2-*g*-P(BpyClCl)) NPs were prepared via surface-initiated ATRP of BpyClCl from the SiO_2-BCl NPs in water at 80 °C for 8 h. The presence of the grafted P(BpyClCl) brushes was confirmed by the XPS Cl 2p, C 1s, and N 1s core-level spectra (Figure 1c,d,d′) of the SiO_2-*g*-P(BpyClCl)) NPs. The peak components at the BE of about 197 and 402 eV[6,9] are attributable to the negatively charged chloride (Cl^-) and positively charged nitrogen (N^+) species, respectively. No nitrogen signal was observed on the preceding SiO_2-BCl NPs (Figure 1b′). The C 1s core-level spectrum (Figure 1d) of the SiO_2-*g*-P(BpyClCl)) NPs can be curve-fitted with four peak components having BEs at about 283.9, 284.6, 285.8, and 286.3 eV, attributable to the C-Si, C-H, C-N, and C-Cl species, respectively.[6,9] The minor peak component of the covalent chloride species in the Cl 2p core-level spectrum (at the BE of about 200 eV, Figure 1c) and the C-Cl species in the C 1s core-level spectrum are associated with the dormant alkyl halide groups preserved throughout the ATRP process. On the basis of the XPS sampling depth of ~7.5 nm (at the photoelectron takeoff angle of 90°) in an organic matrix and the [N]/[Si] ratio (determined from the sensitivity-factor corrected N 1s and Si 2p core-level spectral area ratio),[6] the thickness of the P(BpyClCl) brushes was estimated to be ~5 nm in the dry state. On the basis of the hydrodynamic radius of particles from dynamic light scattering measurements, the thickness of the P(BpyClCl) brushes was ~6.5 nm in the wet state.

Figure 2 shows the UV−visible absorption spectra of an aqueous dispersion of the SiO_2-*g*-P(BpyClCl) NPs before irradiation, after 20 min of UV irradiation, and after 1 min of bleaching in air. No absorption bands were observed in the 400−800 nm wavelength range before irradiation. Upon photoirradiation for 20 min, the dispersion turns faint blue, and two obvious absorption bands have appeared at about 503 and 610 nm. After the irradiation period, the dispersion was exposed to air and allowed to bleach for 1 min. The blue coloration and typical absorption bands disappeared immediately. These characteristics are consistent with those of the BpyClCl monomers (Figure S1, Supporting Information). The color and typical absorption changes resulted from the reversible conversion of dications (BV^{2+}) of the viologen moieties to radical monocations ($BV^{+\cdot}$). Upon UV irradiation, viologen BV^{2+} can be readily reduced to radical $BV^{+\cdot}$ via the transfer of an electron from the counteranion. The resultant $BV^{+\cdot}$ oxidizes readily to the BV^{2+} again by O_2 because of the strong reductive ability of $BV^{+\cdot}$ (Scheme S1, Supporting Information). Therefore, the P(BpyClCl) brushes with BV^{2+} can be "unlocked" by UV irradiation to the $BV^{+\cdot}$ state, whereas the resultant P(BpyClCl) brushes in the $BV^{+\cdot}$ state can be "locked" again to the original BV^{2+} state by exposure to air. The rapid response of the P(BpyClCl) brushes to several cycles of UV irradiation and bleaching in air is shown in the inset of Figure 2. The brushes

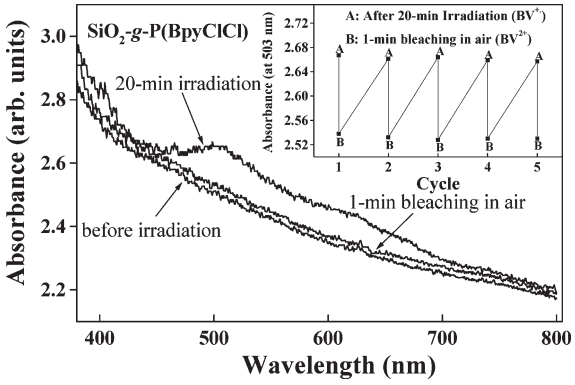

Figure 2. UV−visible absorption spectra of aqueous dispersion of the SiO_2-*g*-P(BpyClCl) NPs (before irradiation, after 20 min irradiation, and 1 min bleaching in air), and the response (inset) of the SiO_2-*g*-P(BpyClCl) NPs subjected to cyclic UV irradiation by monitoring the absorbance at 503 nm.

exhibit a high degree of stability, and after five cycles, the maximum absorbance at 503 nm does not change significantly (< 1%).

Metal Reduction on the SiO_2-*g*-P(BpyClCl) NP Surfaces. Our previous work[11] has shown that the $BV^{+\cdot}$ radical cations reduce metal ions in solution without the addition of any metal reducing agents, with the concomitant oxidation of $BV^{+\cdot}$ back to BV^{2+}. Therefore, it is possible to couple the reduction of metal salts to the interconvertible reduction-oxidiation states of the P(BpyClCl) brushes. Here the P(BpyClCl) brushes on the SiO_2 nanospheres were used as the UV/air-mediated metal reduction agents for the preparation of metal nanodots: (i) the reduction process of the metal ions was actuated by activating the P(BpyClCl) brushes with BV^{2+} via UV irradiation in degassed metal salt solutions and (ii) after a predetermined period, the reduction process was terminated through the introduction of air to produce the metal nanodots (SiO_2-*g*-P(BpyClCl)-metal NPs) (Scheme 1). $AuCl_4^-$ and $PtCl_6^{2-}$ were selected as the model metal ions to produce the Au, Pt, and bimetallic Au/Pt nanodots. The SiO_2-*g*-P(BpyClCl) NPs dispersed in the respective Au, Pt, and Au/Pt ion solutions were exposed to UV irradiation for 20 min and then to air immediately to produce the corresponding SiO_2-*g*-P(BpyClCl)-Au, SiO_2-*g*-P(BpyClCl)-Pt, and SiO_2-*g*-P(BpyClCl)-Au/Pt NPs.

The presence of the reduced metallic Au, Pt, and Au/Pt species was confirmed by the transmission electron microscopy (TEM) images (Figure 3). In comparison with the smooth surfaces of the SiO_2-*g*-P(BpyClCl) NPs, numerous metal dots (< 5 nm) are discernible on these NP surfaces after the metal reduction process. The fact that the nanodots formed on the surfaces cannot be removed during the centrifugation and washing cycles indicate the presence of strong interactions between the nanodots and the P(BpyClCl) brushes. Control experiments using the SiO_2 and SiO_2-BCl NPs were also carried out by the same procedures as the SiO_2-*g*-P(BpyClCl) NPs. No nanodots were observed in the TEM images of the control NPs. In addition, the XPS results of these NPs with nanodots also indicated the successful reduction of the Au and Pt ions and the presence of the reduced metal nanodots.

Figure 4 shows the Au 4f core-level spectrum of (a) the SiO_2-*g*-P(BpyClCl)-Au NPs, Pt 4f core-level spectrum of (b) the SiO_2-*g*-P(BpyClCl)-Pt NPs, and Au 4f and Pt 4f core-level spectra of (c,d) the SiO_2-*g*-P(BpyClCl)-Au/Pt NPs. The Au 4f core-level spectra can be curve-fitted with a dominant spin−orbit split doublet, having BEs at about 84.0 ($4f_{7/2}$) and

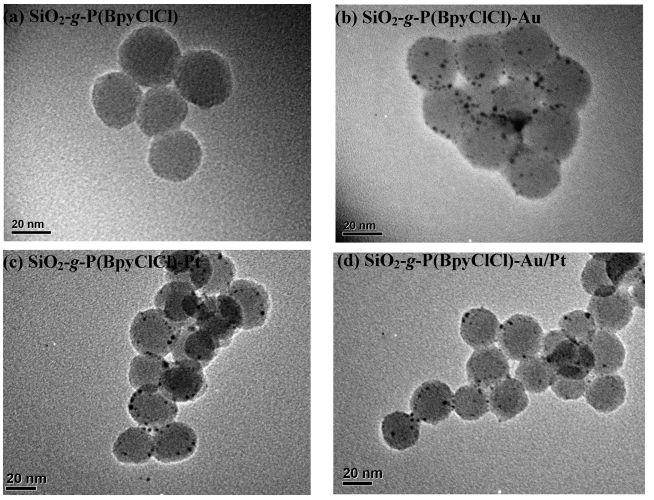

Figure 3. TEM images of the (a) SiO_2-*g*-P(BpyClCl), (b) SiO_2-*g*-P(BpyClCl)-Au, (c) SiO_2-*g*-P(BpyClCl)-Pt, and (d) SiO_2-*g*-P(BpyClCl)-Au/Pt NPs.

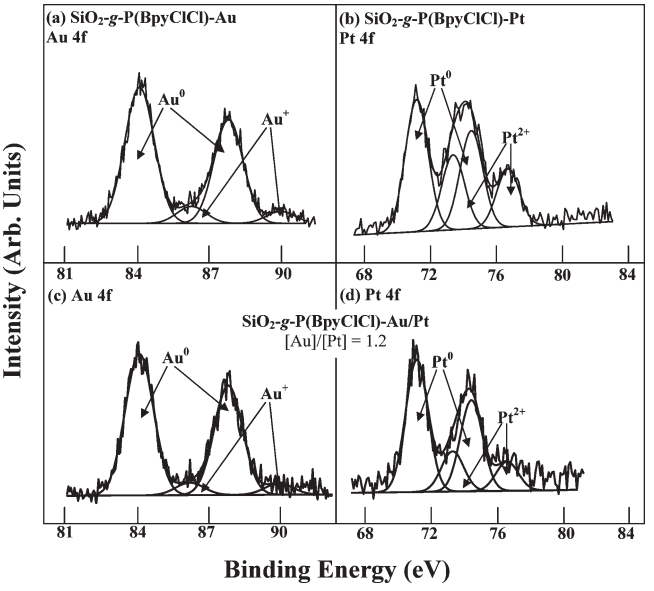

Figure 4. Au 4f core-level spectrum of (a) the SiO_2-*g*-P(BpyClCl)-Au NPs, Pt 4f core-level spectrum of (b) the SiO_2-*g*-P(BpyClCl)-Pt NPs, and Au 4f and Pt 4f core-level spectra of (c,d) the SiO_2-*g*-P(BpyClCl)-Au/Pt NPs.

87.7 ($4f_{5/2}$) eV for the Au^0 species and a minor doublet at 86.1 ($4f_{7/2}$) and 89.8 ($4f_{5/2}$) eV for the Au^+ species.[9] The Pt 4f core-level spectra can be curve-fitted with a major spin−orbit split doublet, having BEs at about 71.2 ($4f_{7/2}$) and 84.5 ($4f_{5/2}$) eV for the Pt^0 species, and a minor doublet at 73.6 ($4f_{7/2}$) and 76.9 ($4f_{5/2}$) eV for the Pt^{2+} species.[9] For the SiO_2-*g*-P(BpyClCl)-Au/Pt NPs, the [Au]/[Pt] ratio of ∼1.2 is slightly higher than that (∼1.0) of the initial metal ions. This phenomenon is consistent with the reduction mechanisms and stoichiometry involved: $AuCl_4^- + 4e^- \rightarrow Au + 4Cl^-$ and $PtCl_6^{2-} + 6e^- \rightarrow Pt + 6Cl^-$. In the control experiments, the pristine SiO_2 and SiO_2−BCl NPs were used instead of the SiO_2-*g*-P(BpyClCl) NPs. No obvious signals associated with Au^0 and Pt^0 species were observed on the NPs after they had been extracted by doubly distilled water and subjected to surface analysis by XPS. These results are thus consistent with the successful reduction of the metal ions on the SiO_2-*g*-P(BpyClCl) NPs.

Conclusions

In summary, novel stimuli-responsive P(BpyClCl) brushes on SiO_2 nanospheres were prepared. The dicationions (BV^{2+}) of the P(BpyClCl) brushes can be reduced upon UV irradiation to become radical monocations ($BV^{+\cdot}$), which revert readily to BV^{2+} by exposure to air. The chemical interconversion of the P(BpyClCl) brushes can be coupled to the metal reduction process for the preparation of metal nanodots-decorated NPs without the addition of any reducing agents. These smart P(BpyClCl) brushes may offer a simple route and added flexibility in the design and preparation of high-surface-area substrates (potential candidates for catalyst) with well-dispersed metal or bimetal species.

Acknowledgment. This work was partially supported by National Natural Science Foundation of China (grant no. 50903007), Research Fund for the Doctoral Program of Higher Education of China (project no. 20090010120007), Program for New Century Excellent Talents in University, and Chinese Universities Scientific Fund (project no. ZZ0904).

Supporting Information Available: Photo- and air-induced interconversion between viologen dication (BV^{2+}) and radical monocation ($BV^{+\cdot}$), UV−visible absorption spectra of aqueous dispersion of the BpyClCl monomers, and FESEM image of the SiO_2−BCl NPs. This material is available free of charge via the Internet at http://pubs.acs.org.

References and Notes

(1) (a) Azzaroni, O.; Moya, S.; Farhan, T.; Brown, A. A.; Huck, W. T. S. *Macromolecules* **2005**, *38*, 10192–10199. (b) Moya, S.; Azzaroni, O.; Farhan, T.; Osborne, V. L.; Huck, W. T. S. *Angew. Chem., Int. Ed.* **2005**, *44*, 4578–4581. (c) Boyes, S. G.; Akgun, B.; Brittain, W. J.; Foster, M. D. *Macromolecules* **2003**, *36*, 9539–9548. (d) Mei, Y.; Sharma, G.; Lu, Y.; Ballauff, M.; Drechsler, M.; Irrgang, T.; Kempe, R. *Langmuir* **2005**, *21*, 12229–12234. (e) Haupt, B.; Neumann, Th.; Wittemann, A.; Ballauff, M. *Biomacromolecules* **2005**, *6*, 948–955. (f) Anikin, K.; Rocker, C.; Wittemann, A.; Wiedenmann, J.; Ballauff, M.; Nienhaus, G. U. *J. Phys. Chem. B* **2005**, *109*, 5418–5420. (g) Houbenov, N.; Minko, S.; Stamm, M. *Macromolecules* **2003**, *36*, 5897–5901. (h) Biesalski, M.; Ruhe, J. *Macromolecules* **2003**, *36*, 1222–1227. (i) Zhang, H.; Ruhe, J. *Macromolecules* **2005**, *38*, 10743–10749. (j) Konradi, R.; Ruhe, J. *Macromolecules* **2004**, *37*, 6954–6961.

(2) (a) Luzinov, I.; Minko, S.; Tsukruk, V. V. *Prog. Polym. Sci.* **2004**, *29*, 635–698. (b) Kumar, N. A.; Seidel, C. *Macromolecules* **2005**, *38*, 9341–9350. (c) Sharma, G.; Ballauff, M. *Macromol. Rapid Commun.* **2004**, *25*, 547–552.

(3) (a) Raveendran, P.; Fu, J.; Wallen, S. L. *J. Am. Chem. Soc.* **2003**, *125*, 13940–13941. (b) Manna, L.; Scher, E. C.; Alivisatos, A. P. *J. Am. Chem. Soc.* **2000**, *122*, 12700–12706. (c) Zhao, M.; Sun, L.; Crooks, R. M. *J. Am. Chem. Soc.* **1998**, *120*, 4877–4878. (d) Mafune, F.; Kohno, J.; Takeda, Y.; Kondow, T. *J. Am. Chem. Soc.* **2003**, *125*, 1686–1687. (e) Wang, R.; Yang, J.; Zheng, Z.; Carducci, M. D.; Jiao, J.; Seraphin, S. *Angew. Chem., Int. Ed.* **2001**, *40*, 549–552.

(4) Yamaguki, H.; Harad, A. *Biomacromolecules* **2002**, *3*, 1163–1169.

(5) Fu, G. D.; Zhao, J. P.; Sun, Y. M.; Kang, E. T.; Neoh, K. G. *Macromolecules* **2007**, *40*, 2271–2275.

(6) (a) Tan, K. L.; Woon, L. L.; Wong, H. K.; Kang, E. T.; Neoh, K. G. *Macromolecules* **1993**, *26*, 2832–2836. (b) Xu, F. J.; Kang, E. T.; Neoh, K. G. *Macromolecules* **2005**, *38*, 1573–1580.

(7) (a) Bird, C. L.; Kuhn, A. T. *Chem. Soc. Rev.* **1981**, *10*, 49–82. (b) Monk, P. M. S. *The Viologens: Physicochemical Properties, Synthesis, and Applications of the Salts of 4,4′-Bipryidine*; John Wiley & Sons: Chichester, U.K., 1998; pp 4−118.

(8) (a) Nanasawa, M.; Miwa, M.; Kuwabara, T. *J. Org. Chem.* **2000**, *65*, 593–395. (b) Kamogawa, H.; Ono., T. *Chem. Mater.* **1991**, *3*, 1020–1023.

(9) Moulder, J. F.; Stickle, W. F.; Sobol, P. E.; Bomben, K. D. In *X-ray Photoelectron Spectroscopy*; Chastain, J., Ed; Perkin-Elmer: Eden Prairie, MN, 1992; pp 41−99.

(10) Husseman, M.; Malmström, E. E.; McNamara, M.; Mate, M.; Mecerreyes, D.; Benoit, D. G.; Hedrick, J. L.; Mansky, P.; Huang, E.; Russell, T. P.; Hawker, C. J. *Macromolecules* **1999**, *32*, 1424.

(11) Yu, W. H.; Kang, E. T.; Neoh, K. G. *Ind. Eng. Chem. Res.* **2004**, *43*, 5194–5202.